Modification Mechanism of Phenol-formaldehyde Resin with Crude Bio-oil by Model Compound Method

Yuxiang Yu [1,2] *, Xiaoqian Qiu [1,2], Chao Li [1,2], Jianmin Chang [3], Defu Bao [1,2]

[1] College of Art and Design, Zhejiang Sci-Tech University, 928 Seconded Avenue, Xiasha High Education Zone, Hangzhou 310018, China

[2] Lab of Material Innovation Design and Intelligent Interaction, Zhejiang Sci-Tech University, 928 Seconded Avenue, Xiasha High Education Zone, Hangzhou 310018, China

[3] College of Materials Science and Technology, Beijing Forestry University, 35 Qinghua East Road, Haidian District, Beijing, 100083, China

* Corresponding authors
E-mail:yuyuxiang0612@zstu.edu.cn(YY)

Abstract

To clarify the modification mechanism of bio-oil for phenol-formaldehyde resin with crude bio-oil (BPF), the bio-oil compounds were simplified by model compound method according to the component distribution. The phenol-formaldehyde resin with bio-oil model compounds (BMPF) were prepared and their basic performance, bonding strength and aging characteristics were determined. The changes on the microstructure and chemical bonds of BMPF were also analyzed by scanning electron microscope, Fourier transform infrared spectroscopy, and nuclear magnetic resonance analysis. Results showed that the components of bio-oil had different influence on the performance and microstructure of BMPF, especially phenols. Structural analysis indicated that the phenols and ketones of bio-oil had positive effects on the synthesis of BMPF, while the aldehydes and acids had negative effects. But all components of bio-oil could improve the aging resistance of BMPF inordinately. These results could provide a basis for the modification of BPF.

Keywords: Modification mechanism; Phenol-formaldehyde resin; Crude bio-oil; Model compound method

Introduction

Phenol-formaldehyde resin (PF) is widely used in wood-based panel because of its excellent bonding strength, thermal stability, and heat resistance, etc. [1,2]. Phenol, as the main raw material for preparing PF, however, comes from fossil sources. With the promotion of global policies on resource shortage and environmental protection, seeking or developing a renewable resource to substitute phenol for preparing PF is becoming more important. Over the

past decade, researchers have successfully produced bio-based PF by replacing phenol with sustainable materials such as lignin [3-6], tannins [7,8], cardanol [9], furfural [10], glyoxal [11] and bio-oil [12-15].

Bio-oil, the main product of the rapid pyrolysis of biomass, has been successfully used in the preparation of PF resin in recent years [16-18]. Compared with petroleum-based PF, bio-oil phenol-formaldehyde resin (BPF) has similar chemical and physical properties [13,19], but a better price competitiveness [20,21]. However, the components of bio-oil are complex, including hundreds of organic components such as phenols, ketones, aldehydes, acids and sugars [17,22]. Some organic components in the bio-oil can participate in the reaction to change the structure of resin, thus affecting the properties [23]. Other components that are not involved in the reaction also have influence on the resin properties as fillers [24,25]. In order to enhance the beneficial effects and reduce the negative effects of bio-oil on resin synthesis, it is of great significance to clarify the specific reaction mechanism of the different components in bio-oil.

Model compound method is a way to use artificial compounds with same or similar structure and function to simplify the complex compound, such as bio-oil. Fortunate et al. [26] used 2-hydroxybenzaldehyde as bio-oil model compound to study the delineate effect of process variables on the catalytic hydrodeoxygenation of bio-oil by computational fluid dynamics. Tran et al. [27] studied the influence of Fe/AC and Ni/gamma-Al_2O_3 catalysts on the hydrodeoxygenation of woody bio-oil using guaiacol as model compound. Wang et al. [28] tried to better understand the aging mechanism of bio-oil by evaluating the aging performance for 39 kinds of bio-oil model compounds, and found that acids played an important role in the aging process, because it could be the reactant in the esterification reaction as well as the catalyst for the polymerization reaction of phenol and aldehyde.

In this study, the bio-oil was simplified into five groups, including phenols, ketones, aldehydes, acids and sugars, according to the component distribution of bio-oil by gas

chromatographic-mass spectrometric (GC-MS) analysis. And the bio-oil model compounds and its component model compounds were formulated by model compound method. The phenol-formaldehyde resin with bio-oil model compounds (BMPF) were prepared and their basic performance, bonding strength and aging characteristics were determined. The changes on the microstructure and chemical bonds of BMPF were analyzed by scanning electron microscope (SEM), Fourier transform infrared spectroscopy (FT-IR), and solid state nuclear magnetic resonance (NMR) analysis.

Materials and Methods

Materials

Bio-oil, an acid liquid (pH 3.5), was obtained by the fast pyrolysis of Larix gmelinii (Rupr.) Kuzen in a fluidized bed at 550 ℃ for 2-3 s by the Lab of Fast Pyrolysis of Biomass and Productive Utilization (Beijing Forestry University, Beijing, China). And the organic components of bio-oil were displayed in Table 1 by GC-MS. Phenol, formaldehyde (aqueous solution, 37 wt.%), sodium hydroxide (NaOH), guaiacol, catechol butanone, cyclopentane dione, vanillin, furfural, D-glucose, acetic acid, phenylacetic acid were supplied by Xilong Chemical Industries, Guangdong, China. Poplar veneers (8 % moisture content, 400 mm × 400 mm × 1.5 mm) were provided by Xinda wooden Co., Ltd., Hebei, China.

Table 1. GC-MS of bio-oil.

Compounds	Molecular Formula	Peak Area (%)
Phenols		**33.42**
Guaiacol	$C_7H_8O_2$	6.52
4-methylguaiacol	$C_8H_{10}O_2$	5.72
Phenol	C_6H_6O	3.16
4-methylcatechol	$C_7H_8O_2$	3.65
Catechol	$C_6H_6O_2$	2.64
P-methylphenol	C_7H_8O	1.44
2-methoxy-4-propylphenol	$C_{10}H_{14}O_2$	1.39
Isoeugenol	$C_{10}H_{12}O_2$	1.39
2-cresols	C_7H_8O	1.20
4-ethylguaiacol	$C_9H_{12}O_2$	1.04
4-ethylresorcinol	$C_8H_{10}O_2$	0.90
3,4-xylenol	$C_{10}H_{12}O_2$	0.88
4-methyl-2- methoxy-6 propenyl phenol	$C_{10}H_{10}O_3$	0.82
Eugenol	$C_{10}H_{12}O_2$	0.74
4-Ethylguaiacol	$C_9H_{12}O_2$	0.69
2-methyl-1,4catechol	$C_7H_8O_2$	0.52
2,6-dimethylphenol	$C_8H_{10}O$	0.39
Trimethylhydroquinone	$C_9H_{12}O_2$	0.33
Ketones		**29.56**
2-Butanone	C_4H_8O	6.25
3-Methyl-1,2-cyclopentanedione	$C_6H_8O_2$	5.89

4,6-dimethyl-2-pyrone	$C_7H_8O_2$	4.22
4-methyl-2(5H)-furanone	$C_5H_6O_2$	3.81
2-propyl-2-ethylcyclohexanone	$C_{11}H_{20}O$	3.30
5-methyl-2-furanone	$C_5H_6O_2$	2.70
Acetovanillone	$C_9H_{10}O_3$	1.54
3-ethyl-2-hydroxy-2-cyclopenten-1-one	$C_7H_{10}O_2$	1.36
2-hydroxy-6-methoxyacetophenone	$C_9H_{10}O_3$	0.49
Aldehydes		**13.45**
Vanillin	$C_8H_8O_3$	7.03
Furfural	$C_5H_4O_2$	2.87
5-acetonyl-2-furaldehyde	$C_8H_8O_4$	2.34
Butanal	C_4H_8O	1.21
Acids		**9.33**
Acetic Acid	$C_2H_4O_2$	7.13
4-hydroxy-3-methoxyphenylacetic acid	$C_9H_{10}O_4$	1.29
2,2-dimethylglutaric acid	$C_7H_{12}O_4$	0.75
Camphoric acid	$C_{10}H_{16}O_4$	0.16
Sugars		**10.05**
D-mannose	$C_6H_{12}O_6$	9.26
β-D-allose	$C_{16}H_{12}O_6$	0.79
Others		**4.19**
2-ethyne	C_6H_{10}	1.43
1,9-decadiene	$C_{10}H_{18}$	1.35
2,4-diacetoxypentanel	$C_9H_{16}O_4$	0.27
Hepty lacetat	$C_8H_{10}O_5$	0.37

2,5-dimethyl-3-hexanol	$C_8H_{12}O$	0.34
N-methylpiperidine	$C_6H_{13}N$	0.43

2.2 Preparation

2.2.1 Preparation of model compounds

According to the results of GC-MS analysis of bio-oil (Table 1), the model compounds of bio-oil were configured (Table 2). The moisture content of bio-oil was calculated as 30 %. The bio-oil and its component model compounds were prepared according to the corresponding proportions in the bio-oil. The formula and naming of bio-oil model compounds were detailed in Table 3.

Table 2. Composition and ratio of Bio-oil model compounds.

Model compound	Composition	Ratio
Phenols	Phenol; guaiacol; catechol	4:1:2
Ketones	Butanone; cyclopentane dione	1:1
Aldehydes	Vanillin; furfural	7:3
Sugars	D-glucose	——
Acids	Acetic acid; phenylacetic acid	5:3

Table 3. Preparation of bio-oil model compounds.

Model compounds	Phenols	Ketones	Aldehydes	Acids	Sugars	Water	Name
Bio-oil model	23%	21%	9%	6%	7%	30%	M1
Phenol-free bio-oil model	——	21%	9%	6%	7%	30%	M2
Ketone-free bio-oil model	23%	——	9%	6%	7%	30%	M3
Aldehyde-free bio-oil model	23%	21%	——	6%	7%	30%	M4
Acid-free bio-oil model	23%	21%	9%	——	7%	30%	M5

2.2.2 Preparation of resins

The BMPF were synthesized according to Yu [13]. The molar ratio of phenol (including bio-oil or bio-oil model compounds) to formaldehyde was 1:2. The substitute rate of bio-oil to phenol was 20 wt.%, and the addition amount of NaOH was 20 wt.% of the mass of phenol. The BPF with bio-oil was denoted as BPF0, and the other BPF with bio-oil model compounds were denoted as BMPF1, BMPF2, BMPF3, BMPF4 and BMPF5 according to the name of bio-oil model compounds.

2.2.3 Preparation of samples

The BMPF plywood and films were prepared according to Yu [13]. After keeping for 48 h in the room, the plywood was sawed into samples with dimension of 100 mm × 25 mm × 3 mm, and 5.3 ± 0.3 g samples were selected as plywood samples. The cured resin films (80 mm × 10 mm × 2 mm) were kept in temperature humidity chamber at 20 ± 2 ℃ and 65 ± 5 % relative humidity for 48 h. The sample with a mass of 1.7 ± 0.2 g was selected as the resin film sample.

2.3 Analysis

2.3.1 Basic performance test

The GC-MS analysis of bio-oil was recorded on a GC/MS-QP system (Shimadzu, Kyoto, Japan) with 20 ℃/min heating rate, 3 min time-duration. An inlet temperature of 250 ℃, a He gas injection volume of 0.5 μL and a flow split-ratio of 50:1 were used for the GC. A junction temperature of 260 ℃, an ion temperature of 220 ℃, an EI source electron energy of 70 eV and a scan range of 29-500 amu were used for MS. The moisture content of bio-oil was calculated by V30 Karl-Fischer moisture meter (Mettler Toledo, Zurich, Switzerland). The pH, viscosity, and solid content of resins were tested by China National Standards GB/T 14074-2013. Each experiment was conducted at least three times under the same conditions, and their average values were reported.

The formaldehyde emission and bonding strength of plywood was evaluated on the basis of China National Standard GB/T 17657-2013. In the test of formaldehyde emission, 10 test specimens (150mm×50 mm), cut from the plywood, were positioned in a 10 L glass desiccator. The emitted formaldehyde was absorbed by a Petri dish filled with 300 ml distilled water, and tested by the ultraviolet spectrophotometer (UV) at 412 nm wavelength. In the test of bonding strength, 12 plywood specimens with dimension of 25 mm × 10 mm × 3 mm were dipped into boiling water for 4 h, dried in 60 ± 3 °C for 20 h, and dipped into boiling water for 4 h, then submersed in cold water for 1 h. Then, the samples were tested with a speed at 10.0 mm/min of the cross head.

2.3.2 Aging test

The plywood and resin film samples were examined by a UV accelerated weathering tester (Yiheng Co., Ltd., Shanghai, China) according to the ASTM G 154. Each 12 h weathering cycle consisted of 8 h of UV exposure at 60 ℃ and 4 h condensation at 50 ℃. The plywood sample number was 6, and the resin film sample number was 3.

2.3.3 Characterization

The scanning electron microscope (SEM) analysis of resin resins were measured by SU8010 SEM (Hitachi, Tokyo, Japan) at 5.0 kV accelerating voltage. The Fourier transform infrared spectroscopy (FT-IR) analysis of resin resins were tested by a Nicolet iS5 FT-IR (Nicolet, Wisconsin, USA) over the range of 400 to 4000 cm^{-1} with a 4 cm^{-1} resolution and 64 scans. The solid state nuclear magnetic resonance (NMR) analysis of resins was acquired at a frequency 100 MHz using JNM-ECZ600R (JEOL, Tokyo, Japan).

3 Results and discussion

3.1 Basic performance

The basic performance of BPF and BMPF is shown in Table 4. The pH value of BMPF were all increased in comparison with BPF0, indicating that the acidity of bio-oil model compound was lower than that of bio-oil. BMPF5 had the highest pH value because of the lack of acid compounds. Compare with BPF0, the viscosity of BMPF decreased, which might be due to the less reactions. The bio-oil model compounds had less substances compare to bio-oil,

which would decrease the number of reactions. Besides, the fewer long-chain substances of bio-oil model compounds also weakened the drag effect. The low viscosity of BMPF2 was due to the lack of phenolic substances, which reduced the crosslinking degree of resin. However, BMPF3 had the lowest viscosity because the ketones were kind of good solvent and could promote the reaction between substances.

As shown in Table 4, the solid content of BMPF1 was higher than that of BPF0, indicating that the bio-oil had a greater negative effect than the bio-oil model compounds. BMPF2 had the smallest solid content, because the phenols in M2 were reduced resulting in the lower polymerization degree. The solid content of BMPF3 was smaller than that of BMPF1, which meant that ketones had a positive effect on the resin polyreaction. The increase in solid content of BMPF4 and BMPF5 indicated that the aldehydes and acids of bio-oil had a negative effect. The acids in bio-oil cloud fall the pH value of system, leading to the decreasing number of multi-substituted hydroxymethyl phenol in the resin addition process, and further reducing the resin crosslinking degree. The active site of formaldehyde is 2, while the reaction activity of other aldehydes was lower than that of formaldehyde. This meant that the other aldehydes would become the terminator of reaction, thus reducing the resin solid content.

It can be seen from Table 4 that the formaldehyde emission of BMPF1 was higher than that of BPF0, indicating that many substances in bio-oil were conducive to reduce the formaldehyde emission. In other words, there were many substances in bio-oil that could react with or adsorb formaldehyde. Besides, the formaldehyde emission of BMPF2-5 was also higher than that of BPF0, indicating that the different components of bio-oil played different positive effect on reducing the formaldehyde emission. Such as phenols can polymerized with formaldehyde,

acids can be esterified with formaldehyde, and ketones can promote the reaction of other substances with formaldehyde.

Table 4. Basic performance of BPF and BMPF.

Resins	Characteristics			
	pH (25℃)	Viscosity (25 ℃, mPa·s)	Solid content (%)	Formaldehyde emission (mg/L)
BPF0	11.10±0.13	322±54	45.93±0.22	0.272±0.021
BMPF1	11.28±0.20	136±33	46.38±0.07	0.387±0.018
BMPF2	11.33±0.07	101±12	43.40±0.10	0.594±0.024
BMPF3	11.32±0.03	98±18	44.80±0.12	0.452±0.032
BMPF4	11.32±0.05	112±25	46.16±0.13	0.539±0.039
BMPF5	11.40±0.04	139±34	46.68±0.30	0.438±0.028

3.2 Bonding strength

The bonding strength and its loss rate of BPF and BMPF plywood prepared are shown in Figure 1 [18]. The bonding strength of BMPF1 plywood was lower than that of BPF0 plywood, indicating that the bio-oil had less influence on the resin system than the bio-oil model compounds. BMPF2 plywood had the lowest bonding strength because the core of PF resin was formed by phenol and formaldehyde, but the total amount of phenolic substances of M2 was the lowest, resulting in a serious decrease of resin polymerization degree. Compared with BMPF1 plywood, BMPF3 plywood had a lower bonding strength, indicating that ketones could

indeed promote the resin reaction. The increased bonding strength of BMPF4 resin plywood meant that the aldehydes in the bio-oil had a negative effect on the bonding strength. This might be due to 1) the aldehydes in bio-oil will compete with formaldehyde for reactive sites; 2) The aldehydes in bio-oil basically have only one active site, which blocked the further increase of resin molecular chain. Compared with BMPF1 plywood, the bonding strength of BMPF5 plywood increased, which was due to the decrease of pH value.

It can be seen from Figure 1 that after 960 h of aging, the loss rate of bonding strength of BMPF1 plywood was higher than that of BPF0 plywood, indicating that except the bio-oil model compounds, the other substances in bio-oil also played a positive role in aging resistance. The biggest bonding strength loss rate of BMPF2 plywood was due to the decrease of phenolic content. Compared with BMPF1 plywood, the bonding strength loss rate of BMPF3 plywood was higher, which was due to the long-chain flexible groups in ketones. As all known, the long-chain flexible groups could effectively improve the toughness of resin. Besides, the increased toughness would reduce the resin layer fractures caused by the stress generated and water-corrosion during aging, thereby improving the aging resistance of resin. The decrease of bonding strength loss rate of BMPF4 and BMPF5 plywood was due to the negative effect from aldehydes and pH value on resin synthesis reaction. However, the bonding strength loss rate of BMPF5 plywood was higher than that of BMPF4 plywood, because the lower pH value cloud reduced the resin solubility, which slightly improved the water resistance.

Fig 1. Bonding strength and its loss rate of BPF and BMPF plywood.

3.3 SEM analysis

The apparent morphology changes of BPF and BMPF films before and after aging are shown in Figure 2 [14,19]. The BMPF films before aging had a smooth surface, and the degree of smoothness was higher than that of BPF0. The reason was that there were some solid particles in the bio-oil, which reduced the smoothness of its solidified surface. Besides, it also showed that the selection of bio-oil model was reasonable, which produced better synthesis reaction and formed a smooth surface after curing. Compared with BMPF2-5, the smoothness of BMPF3 film surface was lower because ketones can act as a good solvent and promote the resin to form a better surface.

It can be seen from Figure 2 that the surface roughness of BPF and BMPF increased obviously after aging for 960 h, and defects such as holes and cracks appeared. Compared with BPF0, BMPF1 film had a higher degree of surface aging. Compared with BMPF1-5, BMPF3 and BMPF2 had a greater aging degree. The reduction of phenolic substances reduced the degree of resin polymerization, thereby weakening the aging resistance. Meanwhile, the lack of ketones reduced the oily substances in the system, resulting in a lower water resistance and a higher degree of surface aging of BMPF2 and BMPF3.

Fig 2. SEM images of BPF and BMPF films before and after aging for 960 h (× 500).

3.4 FT-IR analysis

The FT-IR curves of BPF and BMPF before and after aging for 960 h are displayed in Figure 3, and the attribution of characteristic absorption peaks is shown in Table 5 [12,13,15,29].

As shown in Figure 3, the peak of methylene (CH_2) groups at the region of 2924 cm^{-1} and 2854 cm^{-1}. The content of CH_2 groups can indirectly represent the polymerization degree of PF resin [30,31]. The CH2 groups peak of BMPF1 was stronger than that of BPF0, because the phenolic substance activity of bio-oil model was stronger than that of bio-oil. Compared with the BMPF1, the CH_2 groups peak of BMPF2 was weaker because CH_2 was generated by the reaction of phenols and aldehydes, and the reduction of phenols reduced the CH_2 content in the resin. The weakening of CH_2 groups peak of BMPF3 also confirmed the promoting effect of ketones on resin polymerization. The increased of CH_2 groups peak of BMPF4 and BMPF5 meant that aldehydes and acids in bio-oil have a negative effect on the synthesis of BPF resin. The peak of ether bond (C—O—C) groups at the region of 2924 cm^{-1} and 2854 cm^{-1}. Ether bond is another connecting structure between molecular chains of PF resin, which can also indirectly represent the degree of polymerization of PF resin. Compared with BPF0, the change on ether bond peak of BMPF1-5 was similar to those of CH_2 peak.

After aging for 960 h, the peak of CH_2 and C—O—C groups decreased significantly, indicating that the polymerization degree of resin decreased after aging. Compared with BPF0, the CH_2 peak of BMPF1 decreased significantly. It showed that other substances in bio-oil could reduce the polymerization degree of resin synthesis, but improved the aging property of resin. Compared with BMPF1, the CH_2 groups peak of BMPF2 decreased significantly after aging, which might because resin failed to form a good network structure due to the reduction of phenols, resulting in the reduction of aging resistance. The CH_2 groups peak of BMPF3 weakened the biggest. It might be due to the lack of ketones, which increased the contact area of external environment (water, light and other aging factors), and aggravated the aging degree.

Fig 3. FTIR curves of BPF and BMPF before and after aging for 960 h.

Table 5. Peaks and assignment of FT-IR spectra for BPF.

Wave number (cm^{-1})	Vibration	Assignment
3408	$\nu(\text{—OH})$ [a]	Phenolic OH and aliphatic OH stretching vibration
2923, 2852	$\nu(CH_2)$	Aliphatic CH_2 asymmetric stretching vibration
1604, 1452	$\nu(C=C)$	C=C aromatic ring stretching vibration
1047	$\nu(\text{C—O—C})$	Phenolic C—O—C stretching vibration

[a]ν: Stretching vibration.

3.5 NMR analysis

^{13}C NMR images of BPF before and after aging for 960 h are displayed in Figure 4. The chemical shifts of carbon atoms in each group of BPF resin are shown in Table 6 [18,32]. The carbon spectra of BMPF1-5 and BPF0 were basically similar, indicating that the preparation of bio-oil model compound was reasonable, and the conclusion was the same as that of FT-IR analysis. BPF0 had more substances with C=O structure than BMPF1-5 because there were more kinds of C=O substances in bio-oil. Compared with BMPF1, the values of substituted ortho and para aromatic carbons (139-120 ppm) and methylene bridges (45-27 ppm) of BPF0 were smaller, indicating that other components of bio-oil would still affect the resin synthesis process. However, the value of dimethylene ether bridges (77-68 ppm) increased, which might be due to the presence of ethers in bio-oil. Compared with BMPF1, the values of methylene bridges of BMPF2 and BMPF3 decreased, indicating that phenols and ketones in bio-oil played a positive role in synthesis reaction, while the values of methylene bridges of BMPF4 and

BMPF5 increased, indicating that aldehydes and acids in bio-oil had opposite effects.

After aging for 960 h, the intensity of C=O from carboxylic acids and esters (186-168 ppm) increased, indicating that the aged resin had undergone oxidative aging. The intensity of C=O from aldehydes (220-200 ppm) decreased, indicating that some aldehyde groups were converted to carboxyl or ester groups. The reduction of the substituted ortho and para aromatic carbons meant that the resin network structure was broken after aging, and small molecular substances were formed. The decrease of the intensity of methylene bridges indicated that the molecular chain of resin was broken after aging. Compared with BMPF1, the reduction of the methylene bridge of BPF0 was lower, indicating that the improvement on aging resistance of BPF was the result of the overall interaction of bio-oil molecules. The reduction of methylene bridge of BMPF2-5 was higher than that of BMPF1, which also confirmed this inference.

Fig 4. ^{13}C NMR images of BPF and BMPF before and after aging for 960 h.

Table 6. ^{13}C NMR assignment and quantitative analysis of chemical groups for BPF before and after aging for 960 h.

Chemical group structure	Chemical shirt (ppm)	Calculation											
		Before aging						After aging					
		0[a]	1	2	3	4	5	0	1	2	3	4	5
C=O from aldehydes/ketones	220-200	1.16	1.11	1.09	0.79	0.91	1.05	0.95	0.97	0.82	0.65	0.88	0.94
C=O from carboxylic acids	186-176	0.06	0.05	0.06	0.06	0.06	0.04	0.08	0.09	0.10	0.11	0.08	0.05
C=O from esters	176-168	0.04	0.02	0.03	0.03	0.02	0.01	0.09	0.04	0.08	0.09	0.12	0.08
Phenolic carbon	164-145	1.00	1.00	1.00	1.00	1.00	1.00	1.00	1.00	1.00	1.00	1.00	1.00

Assignment	Chemical shift (ppm)	0	1	2	3	4	5	0	1	2	3	4	5
Substituted ortho and para aromatic carbons	139-120	4.72	5.43	4.52	4.20	5.32	5.60	4.12	4.52	4.24	4.03	4.69	5.04
Dimethylene ether bridges	77-68	0.50	0.46	0.22	0.45	0.39	0.43	0.49	0.41	0.42	0.34	0.37	0.36
Methylol groups	68-60	0.61	0.58	0.43	0.53	0.60	0.53	0.57	0.38	0.39	0.30	0.26	0.26
Benzylamines	60-45	1.19	1.05	1.01	0.90	1.04	1.08	1.12	0.92	0.92	0.71	0.93	0.73
Methylene bridges	45-27	2.55	2.63	2.44	2.47	2.65	2.87	2.43	2.49	2.32	2.30	2.51	2.72

[a] 0: BPF0; 1: BMPF1; 2: BMPF2; 3: BMPF3; 4: BMPF4; 5: BMPF5

Conclusions

Crude bio-oil was used as a phenol substitution to synthesize the BPF resin, and its performance and modification mechanism were analyzed by model compound method. The bio-oil components had different influence on performance and microstructure of BPF. Compared with BMPF1, the bonding strength of BMPF2 and BMPF3 plywood decreased, while the bonding strength of BMPF4 and BMPF5 increased. Structural analysis showed that the CH_2 peak in FT-IR and the methylene bridges intensity in NMR of BMPF2 and BMPF3 were lower than that of BMPF1, while the results for BMPF4 and BMPF5 were opposite. These indicated that the phenols and ketones of bio-oil had positive effects, while the aldehydes and acids had negative effects. After aging for 960 h, compared with BMPF1, the CH_2 peak of BMPF2-5 decreased significantly and the reduction of methylene bridge from BMPF2-5 was higher, which meant that all components of bio-oil could improve the aging resistance of BMPF inordinately. These results could provide a basis for the modification of BPF.

Acknowledgements

References

1. Sarika PR, Nancarrow P, Khansaheb A, Ibrahim T. Bio-based alternatives to phenol and formaldehyde for the Production of Resins. Polymers. 2020 Sep;12(10):2237. https://doi.org/polym12102237

2. Xu Y, Guo L, Zhang H, Zhai H, Ren H. Research status, industrial application demand and prospects of phenolic resin. RSC Adv. 2019 Aug;9:28924-28935. https://doi.org/10.1039/C9RA06487G

3. Gong X, Meng Y, Lu J, Tao Y, Cheng Y, Wang H. A review on lignin-based phenolic resin adhesive. Macromol. Chem. Phys. 2022;2100434. https://doi.org/10.1002/macp.202100434

4. Chen Y, Gong X, Yang G, Li Q, Zhou N. Preparation and characterization of a nanolignin phenol formaldehyde resin by replacing phenol partially with lignin nanoparticles. RSC Adv. 2019 Sep;9: 29255-29262. https://doi.org/10.1039/C9RA04827H

5. Solt P, Rößiger B, Konnerth J, Van Herwijnen H. Lignin phenol formaldehyde resoles using base-catalysed depolymerized Kraft lignin. Polymers. 2018 Sep;10:1162. https://doi.org/10.3390/polym10101162

6. Yang W, Rallini M, Natali M, Kenny J, Puglia D. Preparation and properties of adhesives based on phenolic resin containing lignin micro and nanoparticles: A comparative study. Mater. Design. 2019 Jan;2019,161:55-63. https://doi.org/10.1016/j.matdes.2018.11.032

7. Li JJ, Zhu WJ, Zhang SF, Gao Q, Xia CL, Zhang W, Li JZ. Depolymerization and characterization of Acacia mangium tannin for the preparation of mussel-inspired fast-curing tannin-based phenolic resins. Chem. Eng. J. 2019 Aug;370:420-431. https://doi.org/10.1016/j.cej.2019.03.211

8. Hoyos-Martínez PL, Issaoui H, Herrera R, Labidi J, Charrier-El F. Wood fireproofing coatings based on biobased phenolic resins. ACS Sustain. Chem. Eng. 2021 Jan;9(4):1729-1740. https://doi.org/10.1016/10.1021/acssuschemeng.0c07505

9. Zhang WZ, Jiang N, Zhang TT, Li TS.Thermal stability and thermal degradation study of phenolic resin modified by cardanol. Emerg. Mater. Res. 2020 Mar;9(1):180-185. https://doi.org/10.1680/jemmr.18.00133

10. Sui GH, Cheng YY, Yang XM, Wang XF, Wang ZC. Use of sustainable glucose and furfural in the synthesis of formaldehyde-free phenolic resole resins. J. Appl. Polym. Sci. 2019 Mar;136:47733. https://doi.org/10.1002/app.47732

11. Ballerini A, Despres A, Pizzi A. Non-toxic, zero emission tannin-glyoxal adhesives for wood panels. Hoiz Roh Werkst. 2005 Nov;63:477-478. https://doi.org/10.1007/s00107-005-0048-x

12. Kokten ES, Özbay G, Ayrilmis N. Synthesis of biobased phenolic resins using catalytic pyrolysis oil and its effect on oriented strand board performance. J. Adhesion. 2018

Jun:1-15. https://doi.org/10.1080/00218464.2018.1481400

13. Yu YX, Xu PP, Chang MM, Chang JM. Aging properties of phenol-formaldehyde resin modified by bio-oil using UV weathering. Polymers. 2018 Oct;10:1183. https://doi.org/10.3390/polym10111183

14. Cui Y, Hou XP, Wang WL, Chang JM. Synthesis and characterization of bio-oil phenol formaldehyde resin used to fabricate phenolic based materials. Materials. 2017 Jun;10 (6):668-677. https://doi.org/10.3390/ma10060668

15. Dong FG, Wang MC, Wang ZH. Bio-oil as substitute of phenol for synthesis of resol-type phenolic resin as wood adhesive. Int. J. Chem. React. Eng. 2017 Dec;16:1-7. https://doi.org/10.1515/ijcre-2017-0107

16. Li DB, Zhu LY, Berruti F. Autothermal fast pyrolysis of waste biomass for wood adhesives. Industrial Crops and Products. 2021 Oct;170:113711. https://doi.org/10.1016/j.indcrop.2021.113711

17. Kim J. Production, separation and applications of phenolic-rich bio-oil — a review. Bioresource Technol. 2015 Feb;178:90–98. https://doi.org/10.1016/j.biortech.2014.08.121

18. Celikbag Y, Nuruddin M, Biswas M, Asafu-Adjaye O, Via BK. Bio-oil-based phenol-formaldehyde resin: comparison of weight-and molar-based substitution of phenol with bio-oil. J. Adhes. Sci. Technol. 2020 Jun;34:1-12. https://doi.org/10.1080/01694243.2020.1784540

19. Aalan M, Özbay G, Ayrilmis N. Adhesive characteristics and bonding performance of phenol formaldehyde modified with phenol-rich fraction of crude bio-oil. J. Adhes. Sci,

Technol. 2015 Aug;29:2679-2691.

https://doi.org/10.1080/01694243.2015.1080474

20. Choi G, Oh S, Lee S, Kim J. Production of bio-based phenolic resin and activated carbon from bio-oil and biochar derived from fast pyrolysis of palm kernel shells. Bioresource Technol. 2014 Feb;178:99-107.

https://doi.org/10.1016/j.biortech.2014.08.053

21. Domínguez JC, Oliet M, Alonso MV, Rojo E, Rodríguez F. Structural, thermal and rheological behavior of a bio-based phenolic resin in relation to a commercial resol resin. Ind. Crop. Prod. 2013 Jun;42:308-314.

https://doi.org/10.1016/j.indcrop.2012.06.004

22. Yogalakshmi KN, Devi TP, Sivashanmugam P, Kavitha S, Ravi YK, Varjani SJ, et al. Lignocellulosic biomass-based pyrolysis: A comprehensive review. Chemosphere. 2021 Aug;286:131827. https://doi.org/10.1016/j.chemosphere.2021.131824

23. Usino DO, Ylitervo P, Moreno A, Sipponen MH, Richards T. Primary interactions of biomass components during fast pyrolysis. J. Anal. Appl. Pyrol. 2021 Aug;7:10529.

https://doi.org/10.1016/j.jaap.2021.105297

24. Zhang J, Choi YS, Yoo CG, Kim TH, Brown RC, Shanks BH. Cellulose–Hemicellulose and cellulose–lignin interactions during fast pyrolysis. ACS Sustain. Chem. Eng. 2015 Dec;3:293-301. https://doi.org/10.1021/sc500664h

25. Zhou H, Wu CF, Meng AH, Zhang YG, Williams PT. Effect of interactions of biomass constituents on polycyclic aromatic hydrocarbons (PAH) formation during fast pyrolysis. J. Anal. Appl. Pyrol. 2014 Sep;110:264-269.

https://doi.org/10.1016/j.jaap.2014.09.007

26. Fortunate O, Kishore N. Computational fluid dynamics investigation on catalytic hydrodeoxygenation of a bio-oil model compound in a fluidized bed reactor. J. Therm. Sci. Eng. Appl. 2021 Dec;13:061018. https://doi.org/10.1115/1.4050565

27. Tran QK, Ly HV, Kwon B, Kim SS, Kim J. Catalytic hydrodeoxygenation of guaiacol as a model compound of woody bio-oil over Fe/AC and Ni/gamma-Al$_2$O$_3$ catalysts. Renew. Energ. 2021 Aug;173:886-895. https://doi.org/10.1016/j.renene.2021.03.138

28. Wang R, Ben H. Accelerated aging process of bio-oil model compounds: A mechanism study. Front. Energy Res. 2020 May;8:79. https://doi.org/10.3389/fenrg.2020.00079

29. Yu YX, Xu PP, Chen C, Chang JM, Li LF. Formaldehyde emission behavior of plywood with phenol-formaldehyde resin modified by bio-oil under radiant floor heating condition. Build. Environ. 2018 Aug;144:565-572. https://doi.org/10.1016/j.buildenv.2018.08.025

30. Strzemiecka B, Zieba-Palus J, Voelkel A, Lachowicz T, Socha E. Examination of the chemical changes in cured phenol-formaldehyde resins during storage. J. Chromatogr. A. 2016 Apr;1441:106-115. https://doi.org/10.1016/j.chroma.2016.02.051

31. Pethrick RA. Design and ageing of adhesives for structural adhesive bonding–A review. P. I. Mech. Eng. L-J. Mat. 2014 Feb;229:1-31.
    https://doi.org/0.1177/1464420714522981

32. Fan DB, Li GY, Qin TF, Chu FX. Synthesis and structure characterization of phenol-urea-formaldehyde resins in the presence of magnesium oxide as catalyst. Polymers

2014 Aug;6(8):2221-2231. https://doi.org/10.3390/polym6082221
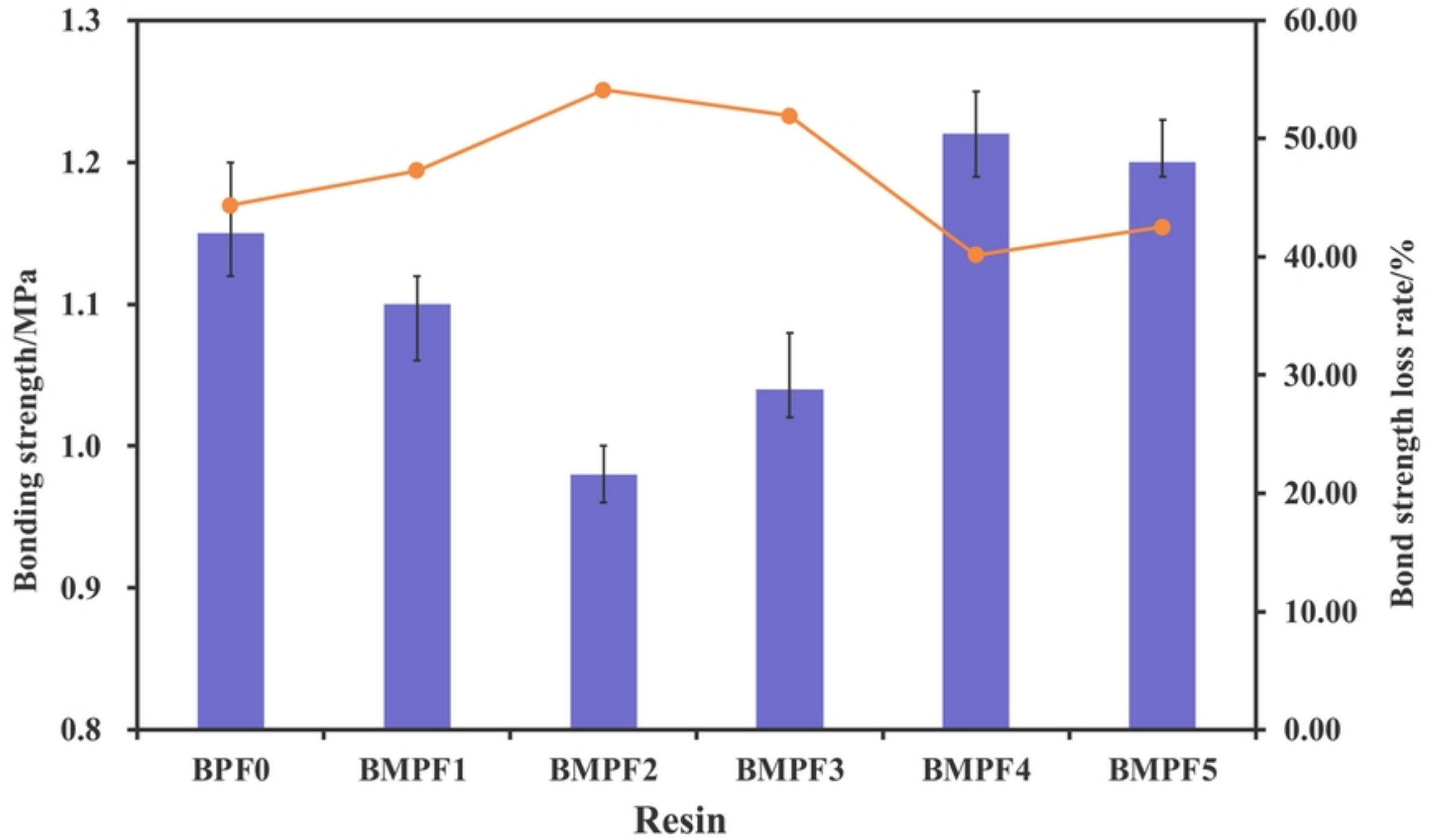
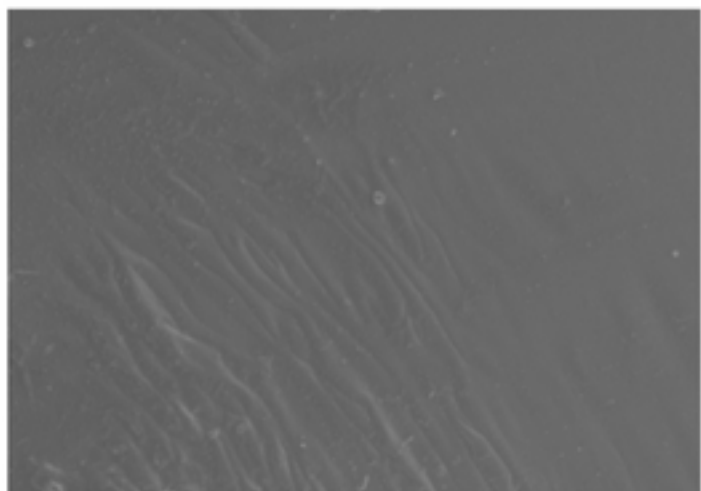Figure 1 Bonding strength and its loss rate of BPF and BMPF plyw
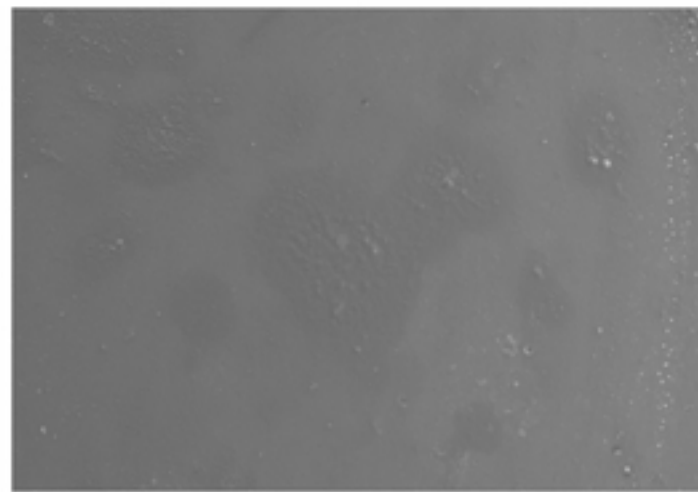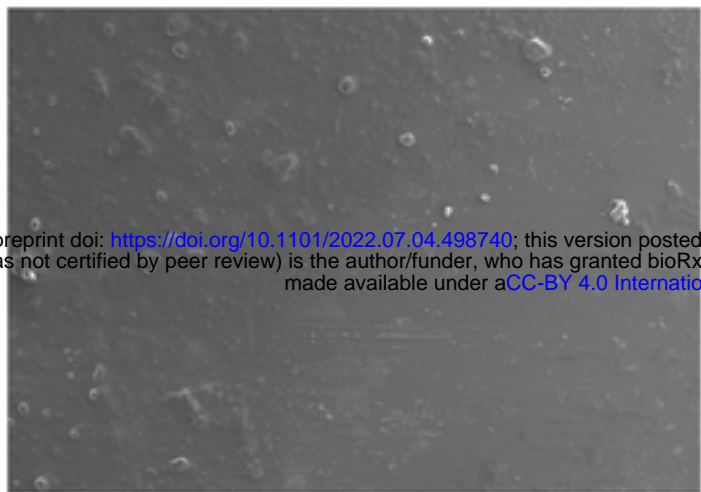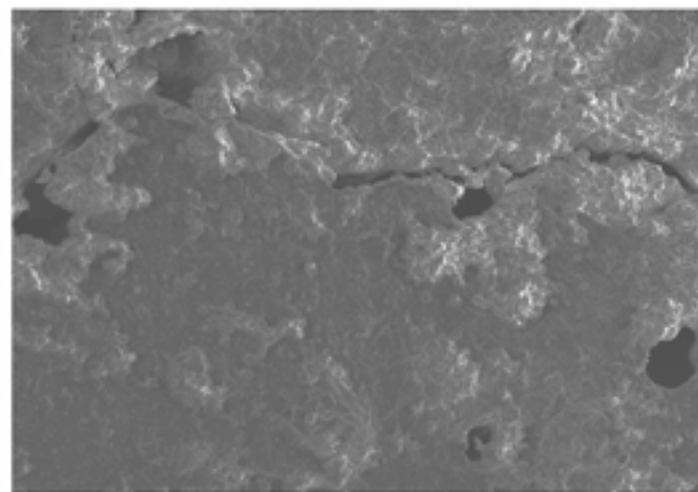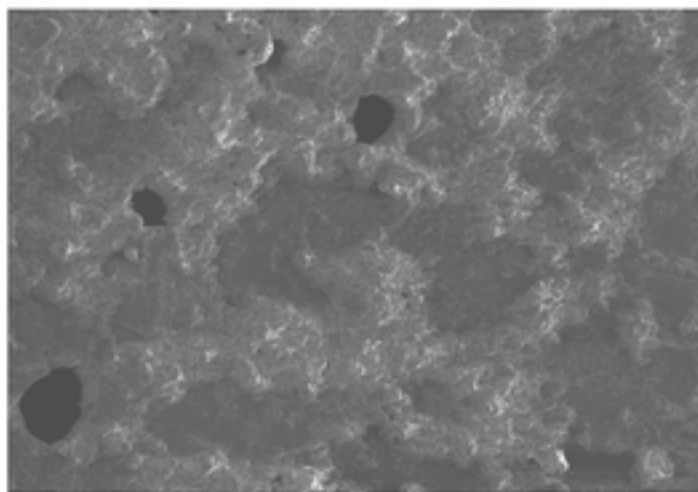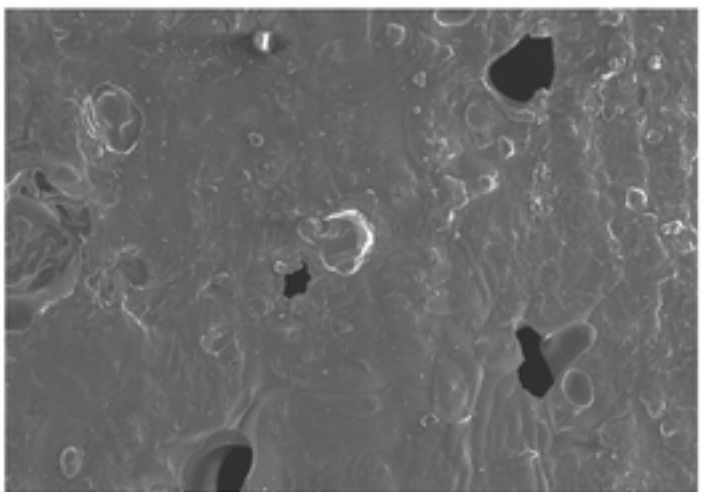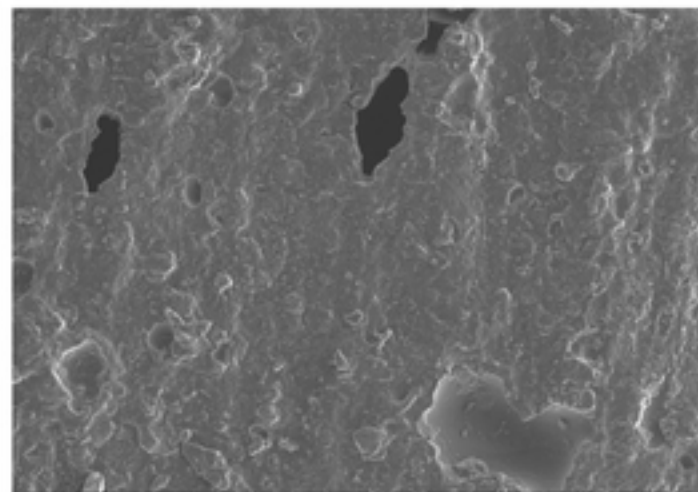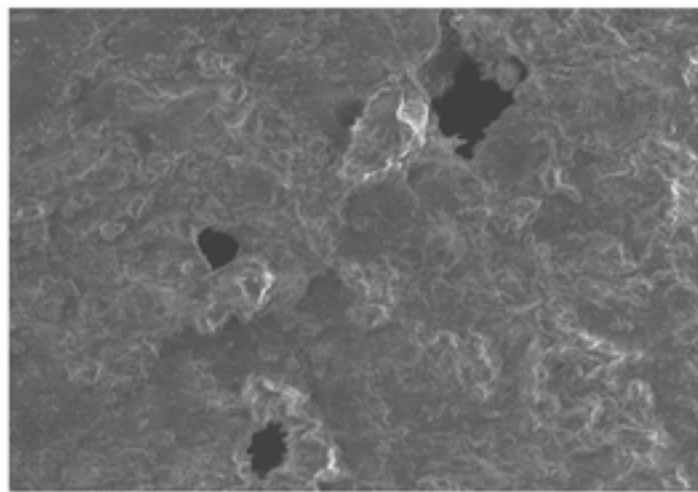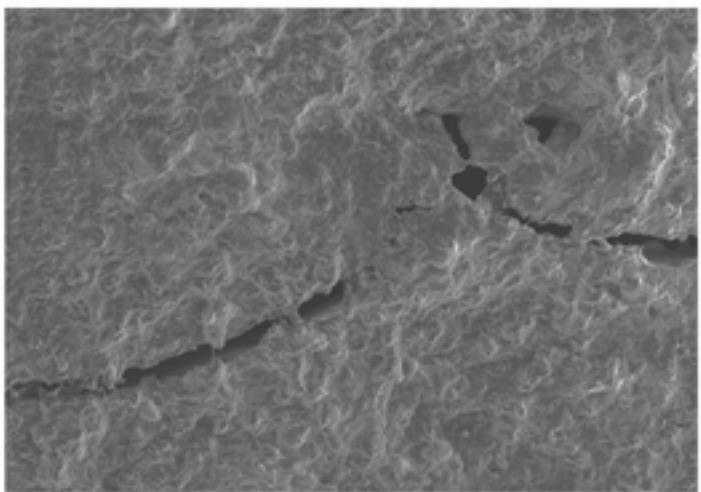
Before

After

BPF0 **BMPF1** **BMPF2**

Before
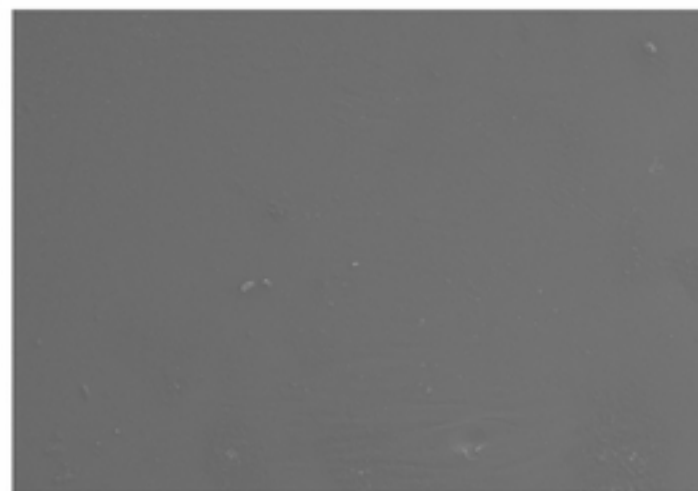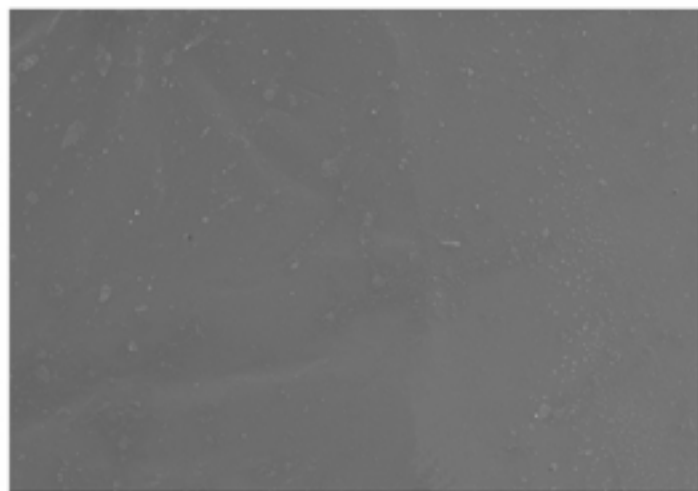
After

BMPF3 **BMPF4** **BMPF5**

Resin

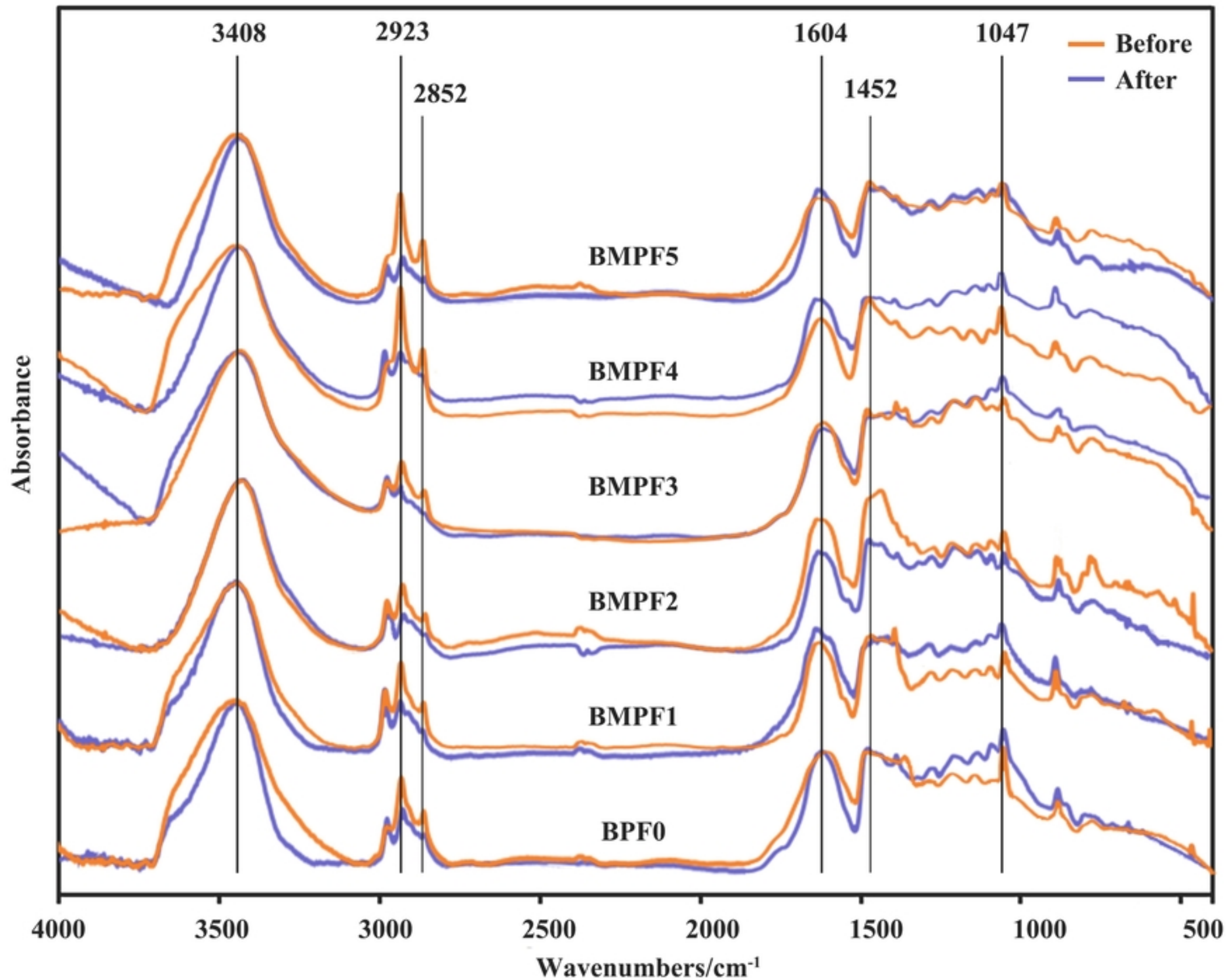Figure 2 SEM images of BPF and BMPF films before and after agi

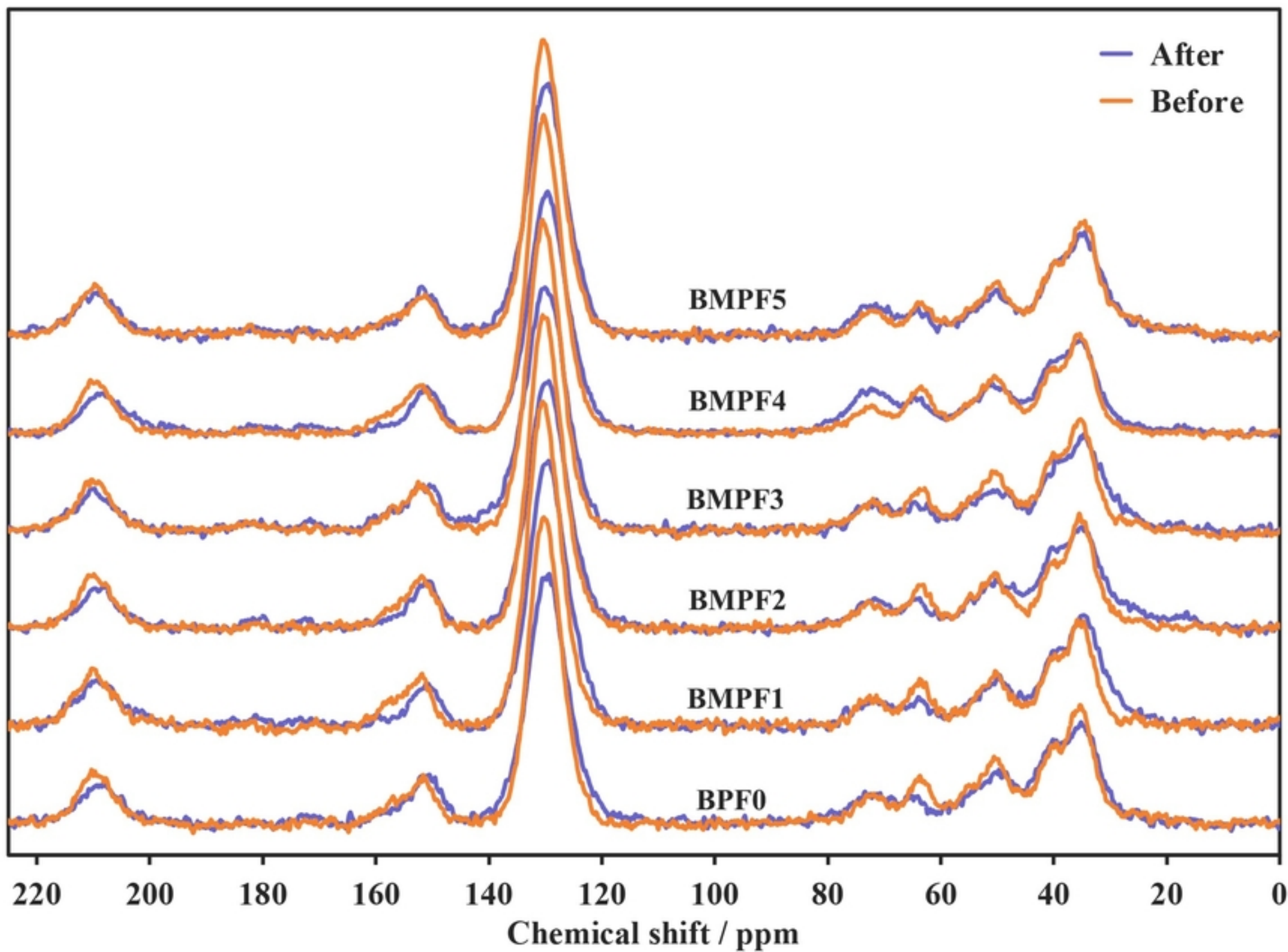Figure 3 FTIR curves of BPF and BMPF before and after aging for

Figure 4 13C NMR images of BPF and BMPF before and after agin